

Relation Learning and Aggregate-attention for Multi-person Motion Prediction

Kehua Qu[†], Rui Ding^{†*}, Jin Tang^{*}

Abstract—Multi-person motion prediction is an emerging and intricate task with broad real-world applications. Unlike single person motion prediction, it considers not just the skeleton structures or human trajectories but also the interactions between others. Previous methods use various networks to achieve impressive predictions but often overlook that the joints relations within an individual (intra-relation) and interactions among groups (inter-relation) are distinct types of representations. These methods often lack explicit representation of inter&intra-relations, and inevitably introduce undesired dependencies. To address this issue, we introduce a new collaborative framework for multi-person motion prediction that explicitly modeling these relations: a GCN-based network for intra-relations and a novel reasoning network for inter-relations. Moreover, we propose a novel plug-and-play aggregation module called the Interaction Aggregation Module (IAM), which employs an aggregate-attention mechanism to seamlessly integrate these relations. Experiments indicate that the module can also be applied to other dual-path models. Extensive experiments on the 3DPW, 3DPW-RC, CMU-Mocap, MuPoTS-3D, as well as synthesized datasets Mix1 & Mix2 (9~15 persons), demonstrate that our method achieves state-of-the-art performance.

Index Terms—Multi-person motion prediction, Relation modeling, Aggregate-attention

I. INTRODUCTION

Human motion prediction (HMP) aims to predict future human motion sequences based on the observed sequences. The HMP plays a major role in many real-world applications, such as autonomous driving [61], [36], robotics [63], [48], surveillance systems [64]. Due to the remarkable development of deep learning, the HMP has made unprecedented progress in recent years [39], [29], [62], [6]. However, single-person motion prediction methods focus solely on intra-relations, which contain the relative positions and movement patterns among body joints (e.g., hip, ankle, wrist) of the same individual. Humans are intuitively social agents, and they continuously interact with other people and their motion may also be influenced by the motions of others. Therefore, multi-person motion prediction task carries more practical significance compared to single-person motion prediction. This task is more challenging because of the sophisticated interactions across different individuals.

Kehua Qu, and Rui Ding are with Information Engineering College, Capital Normal University, Beijing 100048, China. Email: 2221002103@cnu.cn, 5758@cnu.cn.

Jin Tang is with the School of Intelligent Engineering and Automation, Beijing University of Posts and Telecommunications, Beijing 100876, China. E-mail: tangjin@bupt.edu.cn.

*Corresponding authors.

[†]These authors contributed equally to this work.

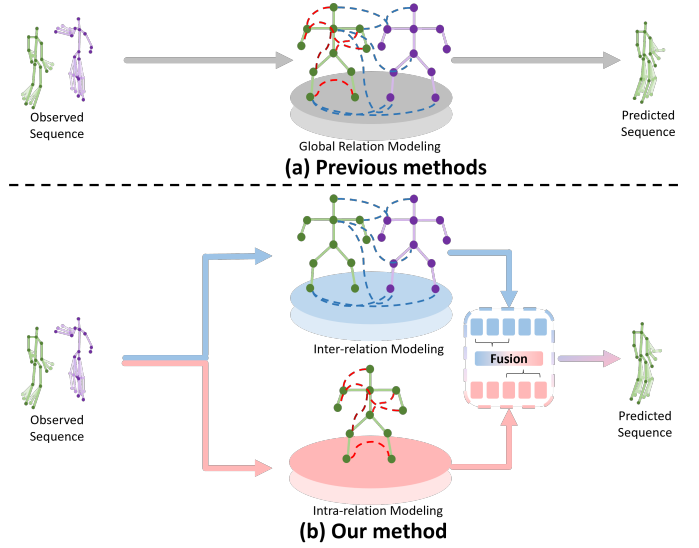


Fig. 1. Compared to previous methods [43], [42], [45], [55] with relation learning, we propose a new collaborative learning framework that explicitly explore joints relations, including intra-relations and inter-relations. The red and blue dashed lines indicate the inter-relation and intra-relation, respectively.

The previous works on multi-person motion prediction generally tend to exploring interactive behaviors by global relation modeling in which all skeleton joints are treated as a whole to establish the relations between them via self-attention [43], [42], [45], [55]. As shown in Fig. 1(a), these methods ignore the distinct representations of inter-relation and intra-relation. Noted that we define inter-relation as the relation of across different individuals' joints, as the blue dash line shown. Corresponding, we define intra-relation as the relations of an individual's joints, as the red dash line shown. By inputting all skeleton joints as a whole into the network, these methods may inevitably introduce undesired relations which weakens the learning effects of interaction information and simplifies the constraints of joints.

To reveal the advantages of explicit representation relations, we conducted some Transformer-based architecture experiments on the CMU-Mocap dataset: (i) The explicit relation modeling adopts cross-attention to learn inter-relations between different individuals' joints, and self-attention to learn intra-relation of each individual's joints. (ii) The global modeling utilizes self-attention to learn all relations of all inputting skeleton joints. Both baselines are based on Transformer architecture. Inspired by methods [3], [4], we employ the Pearson correlation coefficient (PCC) to model the correlation between different people in the observed scene. The calculation can be

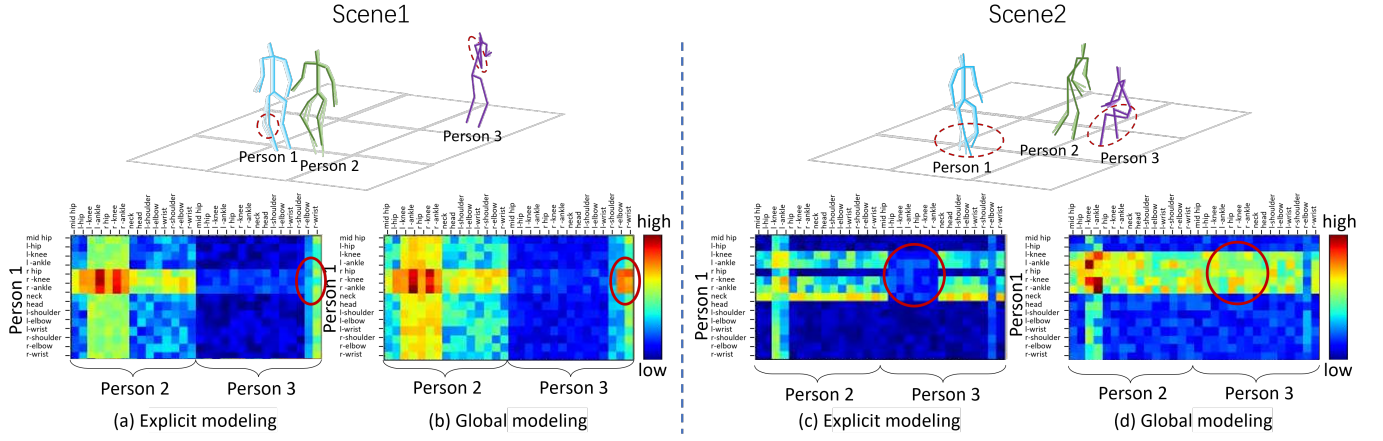


Fig. 2. Visualization of Pearson correlation coefficient (PCC) between different individuals. We conducted two Transformer-based architecture experiments on the CMU-Mocap dataset: (i) The explicit relation modeling adopts cross-attention to learn inter-relations between different individuals' joints, and self-attention to learn intra-relation of each individual's joints. (ii) The global modeling utilizes self-attention to learn all relations of all inputting skeleton joints. For each scene, the upper image shows the true scene in the sequence. The lower image shows the visualization of PCC between the 15 joints of person 1 and the other two persons' joints. The red color indicates higher correlation (larger PCC) between two joints, while the blue indicates lower (smaller PCC).

expressed as follow:

$$PPC(\mathbf{P}_1, \mathbf{P}_2) = \frac{\sum_{t=1}^T (\mathbf{P}_1(t, j) - \bar{P}_1(j))}{\sqrt{\sum_{t=1}^T (\mathbf{P}_1(t, j) - \bar{P}_1(j))^2}} \times \frac{\sum_{t=1}^T (\mathbf{P}_2(t, j) - \bar{P}_2(j))}{\sqrt{\sum_{t=1}^T (\mathbf{P}_2(t, j) - \bar{P}_2(j))^2}} \quad (1)$$

Where \mathbf{P}_n denote the motion representation of n -th person. t denotes the t -th motion sequence and j denotes the j -th skeleton joint. \bar{P}_n denotes the mean value of person n . We visualize PCC between different individuals' joints from two scenes, as shown in Fig. 2. In the first scene, person 1 is walking with person 2. Meanwhile, person 3 is phoning by moving his right arm (in red dashed circle). The red solid circled portions of Fig. 2(a) and Fig. 2(b) indicate the correlation between person 3's right hand and person 1's right leg. (The closer the color is to red, the greater the correlation.) Surprisingly, using the global relation modeling approach, person 3's right hand is correlated with person 1's leg joints, which is not consistent with the fact, as shown in Fig. 2(b). In the second scene, person 2 is conversing with a seated person 3 while person 1 is passing by them. In the observed sequence, there is little correlation between the trajectory of person 1 and the lower body of the stationary person 3 (in red dashed circle). From Fig. 2(c), we can see that the response values between the lower body (hip, knee, ankle) of person 1 and the lower body of person 3 are lower (within the red circle) than those of other body parts. The phenomena demonstrate that the explicit modeling is more effective represent relations and avoid the undesired one. Moreover, global modeling methods make it difficult to assess which parts of the relationships are crucial for prediction accuracy, compromising the model's interpretability.

Therefore, we advocate explicitly modeling relations, as shown in Fig. 1(b). Specifically, we propose a new explicitly modeling framework that contains Graph Convolutional

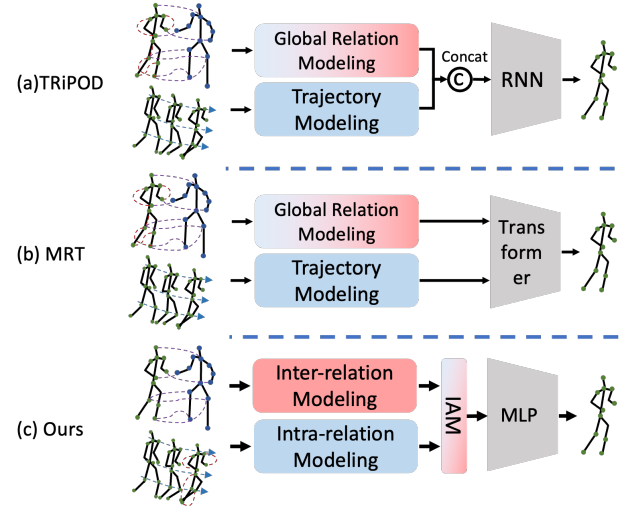


Fig. 3. The illustration of different fusion strategies: (a) TRiPOD [42] concats features from two different branch, then feeds them to an RNN decoder. (b) MRT [43] feeds distinct features to a Transformer decoder to explore their dependency automatically. (c) Our method leverages inter&intra-relations by a designed fusion module (IAM).

Networks (GCN) for intra-relations and the cross-attention attention mechanism for inter-relations. GCN-based methods have surpassed attention mechanism in single-person motion prediction tasks, as demonstrated by references [39], [40], [33], effectively isolating these influences from own joints. In contrast, attention-based approaches excel at handling complex dependencies [16] and prove more effective in multi-person scenarios [43], [44], [45]. In particular, the cross-attention mechanism allows us to exclusively focus on the influence of others (inter-relations) while extracting interaction features, effectively isolating these influences from own joints.

Furthermore, the fusion of intra-relation and inter-relation is critical for high-quality prediction results. Since the simple addition or concatenation operation only mixes the features according to the dimensions [45], [42], it includes too much

irrelevant information to fully extract more helpful information. To tackle the fusion issues, comparing to the previous approaches as shown in Fig. 3, we introduce a novel plug-and-play aggregation module called the Interaction Aggregation Module (IAM), which utilizes a variant attention mechanism that allows one type of relation to directly influence another, ensuring that the fused feature fully takes both types of relationships into account. Moreover, we conduct experiments on several baselines with replacing the our IAM and all these methods achieve improved results. This approach not only improves predictions but also showcases IAM's robust plug-and-play capabilities, as confirmed by our experimental results.

We perform our experiments on multiple datasets, including 3DPW [46], 3DPW-RC [45], CMU-Mocap [51], MuPoTS-3D [52], and synthesized datasets Mix1&Mix2 [43] (9~15 persons). The quantitative results demonstrate that our method achieves state-of-the-art performance.

In summary, our contributions are as follows:

- We propose a collaborative learning framework for multi-person motion prediction to explicitly modeling both the intra-relations within individuals and the inter-relations between them. Explicit modeling clearly illustrate the role of these two relations, enhancing the model's robustness and interpretability.
- We propose a novel plug-and-play aggregation module called the Interaction Aggregation Module (IAM), which introduces an aggregate-attention mechanism to seamlessly integrate intra&inter-relations. Experiments show that this module effectively aggregates these relations and is adaptable to other models requiring integrated information.
- We conduct experiments on several common datasets and our method achieves state-of-the-art performance on all datasets.

II. RELATED WORK

A. Single-Person Motion Prediction.

Early research in single-person motion prediction focused on time series models [32], [1], [38]. Wang et al. [38] propose a novel Position-Velocity Recurrent Encoder-Decoder that effectively utilizes pose velocities and temporal positional information. Despite their success, it seems inappropriate to consider human motion purely as a time series. Human motion involves multiple joint points, each with inherent spatial relationships. For example, the motion relationship between the knee and the ankle differs from that between the elbow and the shoulder. These spatial relationships cannot be captured separately in a time series. To address this issue, GCN-based models are now widely used [39], [40], [33], [6]. Sofianos et al. [40] propose a classic model based on GCN that integrates joint spatio-temporal features. This approach enhances the interaction between body joint connections and their temporal motion patterns, facilitating more effective modeling of human dynamics. Recently, Transformer-based methods have gained widespread attention in the field of motion prediction [31], [30], [29], [62], [2]. Specifically, Aksan et al. [30] employ a

dual-stream architecture based on the Transformer to address both spatial and temporal modeling. However, these methods primarily address single-person scenarios and are unsatisfactory for multi-person tasks.

B. Human-Human/Object Interaction.

Humans are intuitively social agents, they continuously interact with other people and objects. Modeling such interactions has been proven to be effective in various tasks such as 3D human pose estimation [22], [13], [8], human action recognition [18], [25], [49], and human/object trajectory prediction [15], [50], [17].

Cao et al. [50] incorporate scene context (human-object) into motion prediction but overlook human-human interactions, which are more complex due to the dynamic nature of humans compared to static objects. Corona et al. [13] expand the utilization of interactive information in motion prediction, but only limited human-human or human-object correlations are modeled due to the traditional time-series networks. Adeli et al. [49] develop a social context-aware motion prediction framework to capture the interaction between human and human, but the social pooling of method eliminates the characterization of different people's actions. Nevertheless, while these models can capture human-human/object interactions, they cannot be directly applied to HMP due to objectives.

C. Multi-Person Motion Prediction.

Obviously, it does not make sense to divide a multi-person task into multiple single-person tasks [60], [9]. Adeli [42] is the first to consider capturing spatial relations of all persons. Subsequently, more methods [43], [44], [45], [55] devote to considering the human interaction. Parsaeifard et al. [60] use a traditional LSTM [26] encoder-decoder to predict human trajectories, but this approach does not account for crucial interactions between human actions. Adeli et al. [42] adopt GAT [27] to model both people and objects as graph nodes to capture their interactions. Since the attention mechanism of GAT only acts on direct neighbor nodes, the model can capture only local features at each aggregation, making it difficult to directly access global features. This limitation can result in unsatisfactory predictions when global context is crucial. Nowadays, more methods [43], [44], [45], [55], [19] demonstrate the effectiveness of Transformer in this task, as each node can directly focus on all other nodes, not just its neighbors. This capability allows the model to capture global features. Despite these advancements, there is potential for further improvement. Wang et al. [43] employ a local-range Transformer to encode the motion of an individual in the sequence and a global-range Transformer to encode the motion of multiple individuals. Both encoded motions are then sent to a Transformer-based decoder to predict future motion. Guo et al. [19] proposes a novel cross interaction attention mechanism that exploits historical information of both persons, and learns to predict cross dependencies between the two pose sequences. This method primarily focuses on capturing human-to-human interactions and ignore the temporal features modeling, which are equally crucial for accurate prediction.

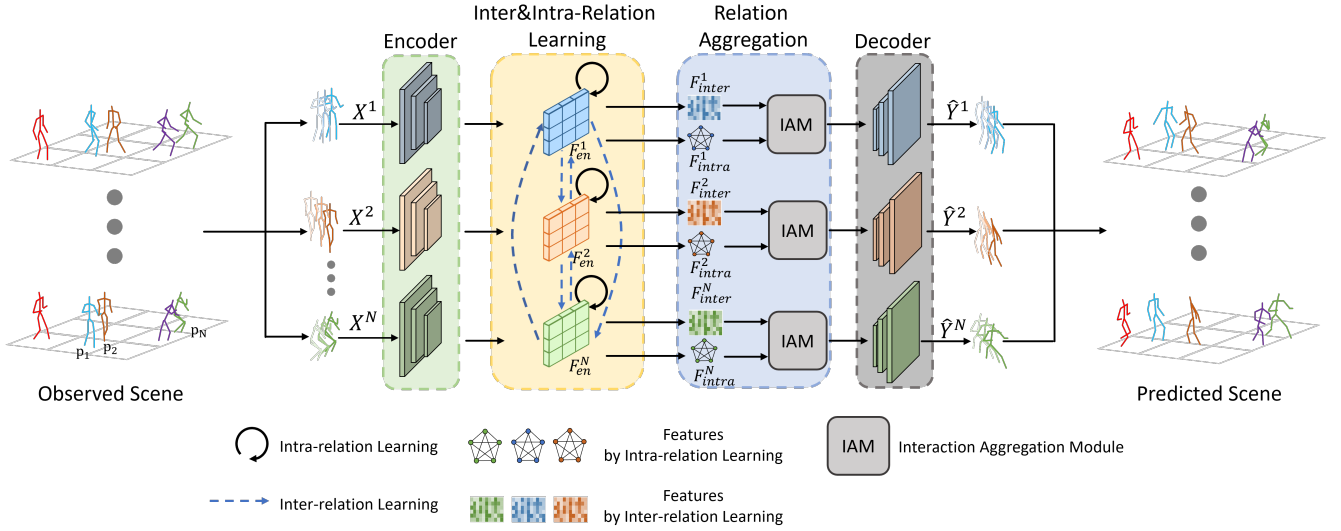


Fig. 4. The architecture of our framework. The method contains : i)Encoder, ii) Intra&inter-relation learning, iii) Relation aggregation, iv)Decoder.

Edward et al. [44] model the interaction between all joints by utilizing the Transformer's attention mechanism. Liu et al. [55] introduce two novel modules to model human trajectories and skeleton joints separately, yet result in the absence of spatio-temporal integration. Xu et al. [45] introduces physical constraints into predictions, indicating that joints connected by bone show stronger associations and that joints belonging to the same individual are related. The above methods treat individuals in a scene collectively when modeling interactions between persons, ignore the distinction between the spatial relationships within a person and those between multiple persons. To address this issue, we introduce a novel framework for capturing intra&inter-relations explicitly.

III. METHODOLOGY

We design a novel and explicit framework for multi-person motion prediction, including encoder-decoder, inter/intra-relation learning and relation aggregation, as shown in Fig. 4.

A. Overview

Given a scene with N persons, each has J skeleton joints, we define the observed sequence of the n -th person as $X^n = \{x_1^n, x_2^n, \dots, x_T^n\}$, where $n \in \{1, 2, \dots, N\}$, N denotes the number of observed people, T represents the observed motion sequence length, and each $x_t^n = (j_{t,1}^n, j_{t,2}^n, \dots, j_{t,J}^n) \in \mathbb{R}^{J \times 3}$ denotes the joints' 3-D coordinates of the n -th person at the t -th motion sequence. Our objective is to predict the future motion sequence of the n -th person, denoted as $\hat{Y}^n = \{\hat{y}_{T+1}^n, \hat{y}_{T+2}^n, \dots, \hat{y}_{T+P}^n\}$, using the observed sequence X^n , where P denotes the predicted motion sequence length. The ground-truth of the n -th person can be defined as $Y^n = \{y_{T+1}^n, y_{T+2}^n, \dots, y_{T+P}^n\}$.

B. Encoder

Instead of using joint position coordinates as input, we utilize the position differences between consecutive time steps

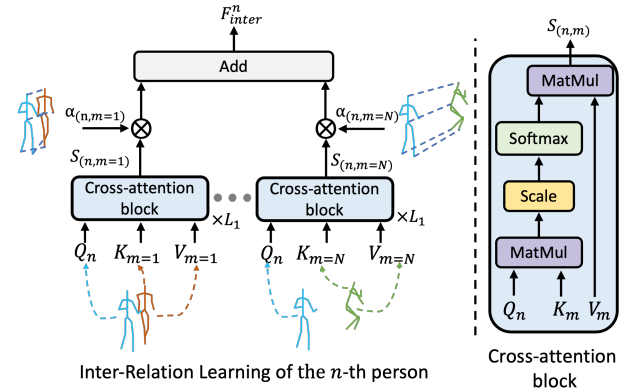


Fig. 5. The illustration of inter-relation learning. The figure above represents the calculation of inter-relation feature of the n -th person. n, m denote two distinct persons, person n and person m . \otimes denotes multiplication.

to represent individual velocities, thereby augmenting the joint information. Each velocity v_t^n is thus expressed as follows:

$$v_t^n = \begin{cases} 0 & (t = 1) \\ x_t^n - x_{t-1}^n & (2 \leq t \leq T) \end{cases} \quad (2)$$

Following this approach, we obtain a new sequence $V^n = \{v_1^n, v_2^n, \dots, v_T^n\}$ as the input of the encoder. The output F_{en}^n of encoder is as follows:

$$F_{en}^n = \text{MLP}(V^n) \quad (3)$$

The MLP block comprises three linear layers, an activation function, and a dropout layer, designed to expand the feature dimensions.

C. Inter/Intra-Relation Learning

1) *Inter-Relation Learning*: To explicitly learn the inter-relation F_{inter}^n among multiple individuals, we introduce a novel module that utilizes cross-attention mechanism. The

overall interaction score for each individual is obtained by weighted summing of the attention scores between that individual and the others, as shown in Fig. 5. The inter-relation feature for the n -th person is calculated as follows:

$$F_{inter}^n = \sum_{m=1}^N \alpha_{(n,m)} \times S_{(n,m)}^{L_1} \quad (n \neq m) \quad (4)$$

The $\alpha_{(n,m)}$ is the weight coefficient in the Eq. 4, and determined by the relative distance between the two individuals. It is calculated as follows:

$$\alpha_{(n,m)} = \frac{1}{\sigma(\lambda) \times \mu \left(\sum_{t=1}^T x_t^n - x_t^m \right) + 1} \quad (5)$$

Where λ is the learnable decay factor, and $\sigma(\cdot)$ is the Sigmoid function, which constrains λ within the range of $0 \sim 1$. μ denotes the average operation. The weight coefficient λ decreases as the distance between the n -th person and the m -th person increases.

The S denotes the score of cross-attention mechanism. We use l to indicate the number of cross-attention blocks, where $l \in \{1, 2, \dots, L_1\}$. The calculation can be expressed as:

$$S_{(n,m)}^l = \begin{cases} \text{ATT}(n, m) & (l = 1) \\ \text{ATT}(S_{(n,m)}^{l-1}, m) & (1 < l \leq L_1) \end{cases} \quad (6)$$

$\text{ATT}(\cdot)$ is the cross-attention mechanism.

$$\text{ATT}(n, m) = MH \left(\text{softmax} \left(\frac{Q^n (K^m)^T}{\sqrt{d_{k^m}}} \right) V^m \right) \quad (7)$$

$MH(\cdot)$ denotes the computing of multi-head attention. Q^n denotes the query of the n -th person, V^m and K^m denote the value and key of the m -th person. $\sqrt{d_{k^m}}$ is the feature size of the key K^m .

2) *Intra-Relation Learning*: In a mean time, we utilize GCN to exploit individual's intra-relations, as shown in Fig. 6. We feed F_{en}^n into the GC-blocks to get the intra-relation information $F_{intra}^n = H^{n, L_2}$.

$$H^{n,l} = \begin{cases} \text{Drop}(\sigma(A^l(BN(F_{en}^n)W^l))) & (l = 1) \\ \text{Drop}(\sigma(A^l(BN(H^{n,l-1})W^l))) & (1 < l \leq L_2) \end{cases} \quad (8)$$

Where l represents the l -th GC-block (in our method $1 \leq l \leq L_2$), and $H^{n,l}$ represents the output of the l -th GC-block of the n -th person. $\text{Drop}(\cdot)$ is a regularization, $\sigma(\cdot)$ is an activation function, and the A^l represents the adjacent matrix of the l -th GC-block. The matrix $A^l \in \mathbb{R}^{C \times C}$ is specifically designed to describe the relationships between nodes in GCN, where $C = J \times 3$ denotes the 3-dimension of J input body joints. $BN(\cdot)$ represents Batch Normalization and W^l is the trainable parameter matrix. Ultimately, we derive the intra-relation features F_{intra}^n of the n -th person.

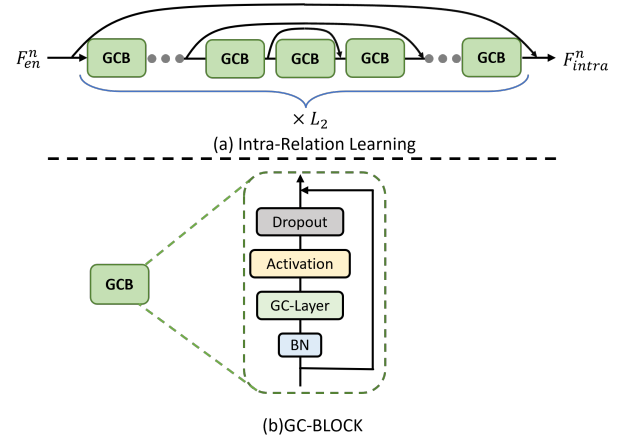


Fig. 6. The illustration of intra-relation learning. (a) We utilize GC-blocks with symmetric residual connection to accomplish intra-relation learning. (b) The architecture of each GC-block.

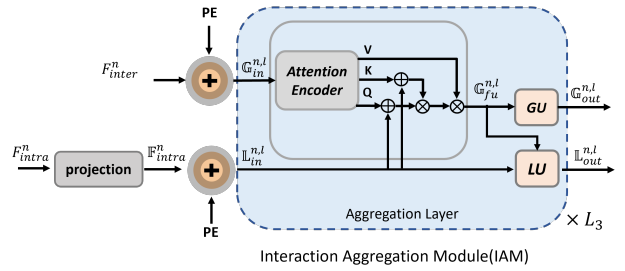


Fig. 7. The computational pipeline of Interaction Aggregation Module (IAM). We introduce an aggregation-attention mechanism to integrate different features from two branches and update both features at each layer.

D. Relation Aggregation

In this section, we introduce a novel feature aggregation module named IAM. It adopts a variant attention mechanism to aggregate intra&inter-relation features, as illustrated in Fig. 7.

To enhance the integration of the two types of relations, we project the intra-relation features into a new dimension, which can be formulated as follows:

$$\begin{aligned} \mathbb{F}_{intra}^n &= \text{PROJ}(F_{intra}^n) \\ &= \sigma(F_{intra}^n \mathbf{W}_1) + \\ &\quad \sigma(\mathbf{W}_2(F_{intra}^n \mathbf{W}_1) \otimes \mathbf{W}_3(F_{intra}^n \mathbf{W}_1)) \end{aligned} \quad (9)$$

Where \mathbf{W}_1 , \mathbf{W}_2 and \mathbf{W}_3 are learnable parameters, \otimes represents Hadamard product.

We then introduce a novel Interaction Aggregation Module (IAM) to enable our predictions to simultaneously utilize both inter&intra-relation features, as shown in Fig. 7:

$$\mathbb{L}_{in}^{n,l} = \begin{cases} \text{PE}(\mathbb{F}_{intra}^n) + \mathbb{F}_{intra}^n & (l = 1) \\ \mathbb{L}_{out}^{n,l-1} & (1 < l \leq L_3) \end{cases} \quad (10)$$

$$\mathbb{G}_{in}^{n,l} = \begin{cases} \text{PE}(F_{inter}^n) + F_{inter}^n & (l = 1) \\ \mathbb{G}_{out}^{n,l-1} & (1 < l \leq L_3) \end{cases} \quad (11)$$

Where “ $\text{PE}(\cdot)$ ” denotes the operation of position encoding. $\mathbb{L}_{in}^{n,l}$ and $\mathbb{G}_{in}^{n,l}$ denotes the input of l -th aggregation layer

of the n -th person, and $\mathbb{L}_{out}^{n,l}$ and $\mathbb{G}_{out}^{n,l}$ denotes the output of l -th aggregation layer of the n -th person. To explicitly incorporate the inter-relations and intra-relations, we design a novel aggregation layer with inter&intra attention mechanism, formulated as:

$$\begin{aligned}\mathbb{G}_{fu}^{n,l} &= \mathcal{F}\left(\mathbb{G}_{in}^{n,l}, \mathbb{L}_{in}^{n,l}\right) \quad (1 \leq l \leq L_3) \\ &= MHA(f_{QKV}(\mathbb{G}_{in}^{n,l}, \mathbb{L}_{in}^{n,l})) \\ &= MH\left(\text{softmax}\left(\frac{(Q^G + \mathbb{L}_{in}^{n,l})(K^G + \mathbb{L}_{in}^{n,l})^T}{\sqrt{d_k}}\right)V^G\right)\end{aligned}\quad (12)$$

Where $MHA(\cdot)$ refers to a variant of multi-head attention. In Eq. 12, we generate the Query/Key/Value for the $\mathbb{G}_{in}^{n,l}$ by the f_{QKV} . We create a special query by adding the embedded intra-relation information $\mathbb{L}_{in}^{n,l}$ to the initial Query derived from the inter-relation Q^G . The resulting features $\mathbb{G}_{fu}^{n,l}$ effectively capture both inter&intra-relations.

Then we update our inter/intra-relations with a global update layer (GU) and a local update layer (LU):

$$\mathbb{G}_{out}^{n,l} = f_{GU}\left(LN\left(\mathbb{G}_{fu}^{n,l}\right)\right) + \mathbb{G}_{in}^{n,l} \quad (13)$$

$$\mathbb{L}_{out}^{n,l} = f_{LU}\left(LN\left(\mathbb{G}_{syn}^{n,l}, \mathbb{L}_{in}^{n,l}\right)\right) + \mathbb{L}_{in}^{n,l} \quad (14)$$

Where $f_{GU}(\cdot)$ is implemented by a MLP block, $f_{LU}(\cdot)$ is consist of a 1-layer Transformer. $LN(\cdot)$ represents Layer Normalization [11].

E. Decoder

After obtaining the refined features \mathbb{G}_{out}^{n,L_3} and \mathbb{L}_{out}^{n,L_3} , we concatenate these and feed them into the decoder:

$$\hat{Y}^n = \mathbf{FC}\left(\text{Concat}\left(\mathbb{G}_{out}^{n,L_3}, \mathbb{L}_{out}^{n,L_3}\right)\right) \quad (15)$$

Following this step, we can finally get the prediction \hat{Y}^n of the n -th person.

F. Loss functions

We define the final loss function \mathcal{L} as the sum of \mathcal{L}_p and \mathcal{L}_v to train the model jointly. The final loss function can be expressed as follows:

$$\begin{aligned}\mathcal{L} &= \mathcal{L}_p^2 + \mathcal{L}_v^2 \\ &= \left[\ell_2\left(\hat{Y}^n, Y^n\right)\right]^2 + \left[\ell_2\left(\hat{Y}_v^n, Y_v^n\right)\right]^2\end{aligned}\quad (16)$$

\mathcal{L}_p aims to minimize the ℓ_2 -norm between the predicted motion \hat{Y}^n and ground-truth Y^n . \mathcal{L}_v aims to minimize the ℓ_2 -norm between the predicted motion \hat{Y}_v^n and ground-truth of velocity Y_v^n calculated by position difference.

IV. EXPERIMENT AND DISCUSSIONS

A. Baselines

We select a range of base models to verify the effectiveness of our method, including classical approaches such as LTD [59], TRiPOD [42], DViTA [60], and MRT [43], the single-person motion prediction method TCD [20], as well as state-of-the-art models JRT [45] and TBIFormer [5] as our

baselines. LTD [59] is a foundational model in the field of human motion prediction that encodes temporal information by operating in trajectory space. TRiPOD [42] first models interactions in human-to-human and human-to-object. DViTA [60] divides multi-person prediction tasks into several single-person prediction tasks. MRT [43] emphasizes the importance of interaction in multi-person prediction tasks by adopting a multi-range Transformer. JRT [45] explores the physical relations of the human body in conjunction with interactions to yield noteworthy outcomes. TBIFormer [5] addresses the human-to-human interactions by focusing on skeletal body parts. It converts all pose sequences into Multi-Person Body-Part sequences, utilizing these transformed sequences to learn the dynamics of body parts for both inter- and intra-individual interactions.

B. Datasets

We adopt four multi-person motion prediction benchmarks in the experiments: 3DPW [46], 3DPW-RC [45], CMU-Mocap [51], MuPoTs-3D [52] and synthesized datasets Mix1&Mix2 [43]. Details of the four datasets are presented below.

3DPW [46] 3D Poses in the Wild Dataset (3DPW) is a large-scale 3D motion dataset collected by moving mobile phone cameras. It contains 60 videos and about 68,000 frames covering multiple scenarios and actions. In this paper, we follow the setting of [28], [42], [55], [45]. Each scene contains two persons, and our goal is to predict future 900ms (14 frames) motion using the historical 1030ms (16 frames) motion.

3DPW-RC [45] According to the findings from the Joint-Relation Transformer [45], camera movement in the 3DPW dataset induces a significant unnatural drift, negatively impacting the modeling of multi-person interactions. The 3DPW-RC dataset subtracts the estimated camera velocity for better evaluation.

CMU-Mocap [51] The Carnegie Mellon University Motion Capture Database (CMU-Mocap) consists of data from 112 subjects. Most scenes capture the movements of one person, and only 9 scenes include the movements and interactions of two persons. The study in [43] combines samples from both one-person and two-person scenes to create sequences featuring three individuals. We use the training and test sets provided by Wang et al. [43] to train and evaluate our model. We aim to predict future 3000ms (45 frames) motion using the historical 1000ms (15 frames) motion.

MuPoTS-3D [52] Multiperson Pose Test Set in 3D (MuPoTS-3D) consists of over 8000 frames collected from 20 sequences with 8 subjects. Following previous works [43], [45], we evaluate our model's performance with the same segment length as CMU-Mocap on the test set.

Mix1&Mix2 [43] In order to evaluate the performance of our proposed model in scenarios involving a larger number of individuals, we adopt the methodology presented in the MRT [43] paper. We sample data from the CMU-Mocap and Panoptic [21] datasets to generate the Mix1 training set. This training set contains approximately 3,000 samples, each featuring 9 to 15 people in the scene. Next we combine CMU-

TABLE I

EXPERIMENTAL RESULTS IN VIM ON 3DPW AND 3DPW-RC TEST SETS. THE BEST RESULTS ARE HIGHLIGHTED IN BOLD. "-" INDICATES THAT THE DATA ARE NOT GIVEN IN THE PAPER AND CANNOT BE REPRODUCED WITHOUT CODE. "*" INDICATES THAT THE DATA ARE NOT GIVEN IN THE PAPER AND WE REPRODUCED WITH THE PAPER'S CODE.

Method	3DPW (2 persons)						3DPW-RC (2 persons)					
	AVG	100	240	500	640	900	AVG	100	240	500	640	900
LTD [59]	76.7	22.0	41.1	81.0	100.2	139.7	62.2	20.2	37.2	68.6	81.3	103.5
TRiPOD [42]	84.2	31.0	50.8	84.7	104.1	150.4	-	-	-	-	-	-
DViTA [60]	65.7	19.5	36.9	68.3	85.5	118.2	57.4	15.0	32.3	62.7	76.3	100.6
MRT [43]	59.2	21.8	39.1	65.1	75.9	94.1	52.3	20.8	36.4	58.2	66.6	79.4
TCD* [20]	51.0	10.8	24.8	55.1	68.3	96.1	43.3	10.2	26.3	50.1	57.8	72.1
TBIFormer* [5]	48.4	9.8	22.5	50.6	63.1	94.2	41.5	9.7	24.0	47.7	55.3	70.8
JRT [45]	47.2	9.5	22.1	48.7	62.8	92.8	39.5	9.5	21.7	44.1	53.4	68.8
Ours	46.5	9.3	21.5	47.3	62.1	92.3	39.0	9.2	21.6	43.6	52.6	68.5

TABLE II

EXPERIMENTAL RESULTS IN MPJPE ON CMU-MOCAP (LEFT) AND MUPOTS-3D (RIGHT) TEST SETS. THE BEST RESULTS ARE HIGHLIGHTED IN BOLD. "*" INDICATES THAT THE DATA ARE NOT GIVEN IN THE PAPER AND WE REPRODUCED WITH THE PAPER'S CODE.

Methods	CMU-Mocap (3 persons)			MuPoTS-3D (2~3 persons)		
	1s	2s	3s	1s	2s	3s
LTD [59]	13.7	21.9	32.6	11.9	18.1	23.4
HRI [31]	14.9	26.0	30.7	9.4	16.8	22.9
TCD* [20]	10.2	16.1	19.5	9.0	15.8	21.7
MRT [43]	9.6	15.7	21.8	8.9	15.9	22.2
TBIFormer* [5]	8.0	13.4	19.0	8.7	15.1	20.9
JRT [45]	8.3	13.9	18.5	8.9	15.5	21.3
Ours	7.8	12.8	16.9	8.5	14.7	20.1

TABLE III

EXPERIMENTAL RESULTS IN MPJPE ON MIX1 (LEFT) AND MIX2 (RIGHT) TEST SETS. THE BEST RESULTS ARE HIGHLIGHTED IN BOLD. "*" INDICATES THAT THE DATA ARE NOT GIVEN IN THE PAPER AND WE REPRODUCED WITH THE PAPER'S CODE.

Methods	Mix1 (9~15 persons)			Mix2 (11 persons)		
	1s	2s	3s	1s	2s	3s
LTD [59]	21.0	31.9	41.5	17.2	25.8	34.5
HRI [31]	18.0	31.4	42.1	16.0	27.1	36.7
MRT [43]	17.3	29.9	39.7	12.9	20.9	28.2
TBIFormer* [5]	14.0	24.4	31.2	12.3	18.2	26.1
Ours	13.7	23.7	29.7	11.8	17.5	25.2

Mocap, MuPoTS-3D and 3DPW data, namely Mix2. There are 11 persons in each scene of its 400 samples.

C. Implementation Details

In practice, for the 3DPW and 3DPW-RC datasets, we set the input length $T = 16$, the output length $P = 14$, and the number of person $N = 2$. For the CMU-Mocap and MuPoTS-3D datasets, we set $T = 15$, $P = 45$ and $N = 3$.

Our model consists of $L_1 = 4$ cross-attention blocks with $H = 8$ attention heads for inter-relation learning, $L_2 = 13$ GC-blocks for intra-relation learning, and $L_3 = 4$ aggregation layers in the IAM. We pre-train the model on the AMASS [58] dataset following previous works [45], [44], which provides massive motion sequences. We utilize the PyTorch deep learning framework to develop our models and optimize the training with AdamW [53] optimizer. The learning rate is set to 1×10^{-5} for both pre-train and finetune and decay by 0.8

every 10 epochs. The batch size is set to 256 for pre-train, 128 for finetune. The training is performed on an NVIDIA 3080Ti GPU for 100 epochs.

D. Metrics

VIM [42] We adopt the Visibility-Ignored Metric (VIM) to measure the displacement in the joint vector, which has a dimension of $J \times 3$, following previous works. This metric is used on the 3DPW and 3DPW-RC datasets.

$$\text{VIM@t} = \frac{1}{N} \sum_{n=1}^N \sqrt{\sum_{j=1}^J (Y_{nj}^t - \hat{Y}_{nj}^t)^2} \quad (17)$$

MPJPE [41] Mean Per Joint Position Error (MPJPE) is a commonly used metric in human motion prediction, which calculates the average Euclidean distance between the prediction and the ground truth of all joints. We use this metric on CMU-Mocap and MuPoTS-3D.

$$\text{MPJPE} = \frac{1}{P} \frac{1}{N} \frac{1}{J} \sum_{t=1}^P \sum_{n=1}^N \sum_{j=1}^J \|Y_{nj}^t - \hat{Y}_{nj}^t\|_2 \quad (18)$$

E. Quantitative Results

1) Results on 3DPW and 3DPW-RC: For a fair comparison, we follow the same VIM criterion as established in previous works [60], [45], [47], [43], [42]. The experimental results in VIM on the 3DPW and 3DPW-RC datasets are shown in Table.I, where our method achieves the best performance on each dataset. Compared to the current state-of-the-art method Joint-Relation Transformer [45], our method reduces the VIM on AVG from 47.2 to 46.5 on 3DPW dataset and from 39.5 to 39.0 on 3DPW-RC dataset. These improvements demonstrate the effectiveness of our method. Traditional single-person motion prediction methods DVITA [60] and LTD [59] focuses on trajectory and ignores human interaction in multi-person motion prediction, so their experimental results are uncompetitive compared to subsequent methods. TRiPOD [42] employs GAT [27] to capture the connections between different targets. However, GAT is limited to capturing local information, as it performs attention operations only on adjacent nodes, thus failing to capture global information. MRT [43] utilizes a multi-range Transformer to model interactions

Fig. 8. Experimental results in VIM on 3DPW test sets. We verify the effectiveness of IAM incorporating different base models, TRiPOD [42], MRT [43], and JRT[45]. The best results are highlighted in bold. "+" denotes base models enhance with our IAM. "⊕" indicates that the fusion module is replaced with our IAM.

Method	3DPW					
	AVG	100	240	500	640	900
TRiPOD [42]	84.2	31.0	50.8	84.7	104.1	150.4
TRiPOD+IAM	77.9	28.6	46.8	79.2	95.1	140.2
MRT [43]	59.2	21.8	39.1	65.1	75.9	94.1
MRT+IAM	54.3	18.1	32.3	59.9	68.2	93.2
JRT [45]	47.2	9.5	22.1	48.7	62.8	92.8
JRT⊕IAM	46.8	9.5	21.8	48.1	62.5	92.8
Ours (w/o IAM)	48.0	9.5	22.4	49.1	64.8	94.5
Ours	46.5	9.3	21.5	47.3	62.1	92.3

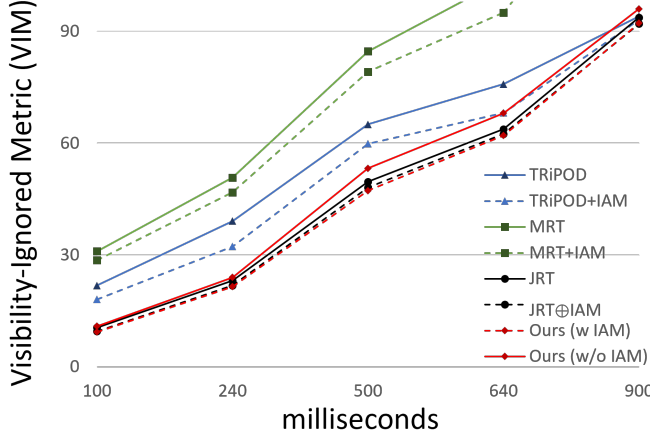


Fig. 9. The line chart of experimental results on the 3DPW [46] dataset. The green line denotes baseline model MRT [43]. The blue line denotes baseline model TRiPOD [42]. The purple line denotes baseline model JRT [45]. The red line denotes our method without IAM. The green, blue, and purple dashed lines denote the baseline models enhanced with our IAM. The red dashed line denotes our method with IAM. Obviously, the utilization of our IAM yields a more accurate prediction.

and human trajectories separately, it employs a Transformer decoder instead of designing a module to aggregate two types of information. Since TCD [20] is designed for single-person motion prediction, it lacks the capability to capture human-to-human interactions. The results highlight the significance of modeling interactions in multi-person motion prediction.

2) *Results on CMUMocap, MuPoTS3D and Mix1&Mix2:* We also compare the results in MPJPE on the CMU-Mocap and MuPots-3D datasets between our method and several other approaches, including MRT [43] and Joint-Relation Transformer [45], as well as two single-person motion prediction methods: HRI [31] and LTD [59]. We provide 15 observed frames (1s) as input to predict the subsequent 45 frames (3s), and report the MPJPE at 1, 2, and 3 seconds into the future, as shown in Table. II. Our method achieves state-of-the-art results on CMU-Mocap and MuPots-3D, demonstrating its accuracy and strong generalization capabilities. In addition, we conduct experiment on the Mix1&Mix2 datasets to validate our method's ability to handle sophisticated scenes involving more than 9 persons, as shown in Table. III. The results demonstrate that our method excels at managing more complex situations.

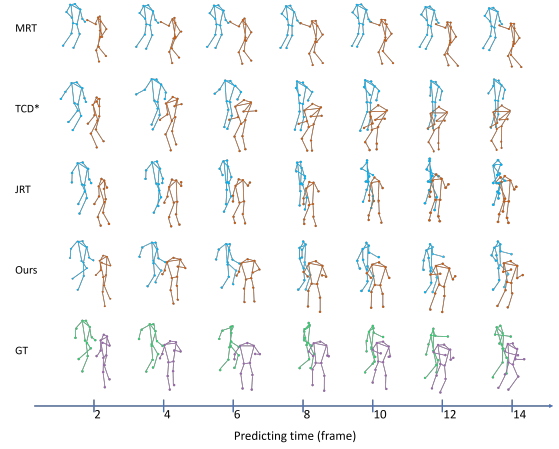


Fig. 10. Visualization comparison on 3DPW-RC dataset. We compare the prediction by our method and three previous methods. Our method generates a more precise motion prediction.

3) *Effectiveness of IAM:* In order to verify the effectiveness of IAM, we designed an study on the 3DPW test set using DViTA [42], MRT [43], and JRT[45] as the base models. The experimental results are shown in Table. 8 and Fig. 9. In these presentations, "TRiPOD+IAM" and "MRT+IAM" refer to the DViTA [42], MRT [43] enhanced with our IAM module. In addition, we replace the fusion module of JRT[45] with our IAM, denotes as "JRT⊕IAM". The results indicate that our IAM provides improvements to the base models, reducing the average error from 84.2 to 77.9 for TRiPOD, from 59.2 to 54.3 for MRT, and 47.2 to 46.8 for JRT. The results confirm that IAM effectively aggregates features from two different branches. These outcomes verify the strong ability of plug-and-play. Additionally, an ablation study was conducted to assess the impact of removing IAM from our method and the results demonstrate the importance of IAM.

F. Qualitative Results

1) *Visualization of prediction result:* We provide a qualitative comparison on 3DPW-RC test set between our method and other recent methods, including MRT [43], FutureMotion [47] and JRT [45], as shown in Fig. 10. Compared with the prediction of FutureMotion [47], MRT [43], and JRT [45], our results are more natural and closer to the ground truth, particularly in the movement of the lower limbs. We also provide the visualization results on CMU-Mocap dataset to verify our method's effectiveness on scenes of 3 persons as shown in Fig. 11. We can notice that both LTD [59] and MRT [43] generate unnatural arm distortions that do not appear in our approach, as shown in the red circles. The visualization results on different datasets demonstrate the generalization and accuracy of our method.

2) *Visualization of attention scores:* We visualize the learned attention matrices in the first layer to demonstrate the effectiveness of the intra-relation learning and inter-interaction learning, as shown in Fig. 12. We observe that in Fig. 12(a) the values between "left foot and right foot" for person 1 and "right foot and knee" for person 2 are significantly

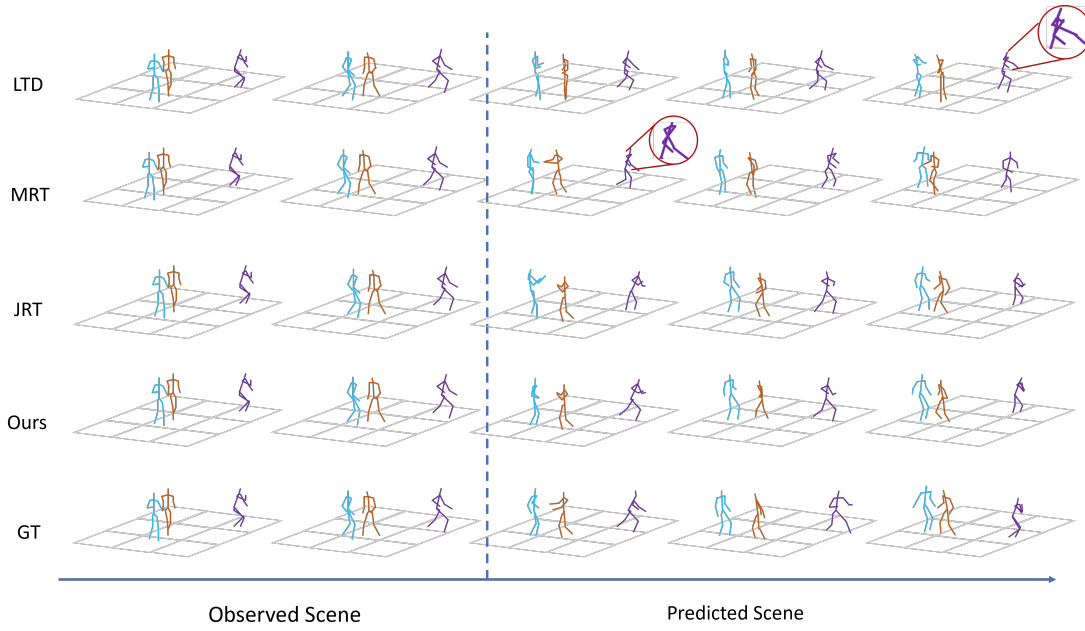


Fig. 11. Visualization comparison on CMU-Mocap dataset. We compare the prediction by our method and three previous methods. Our method generates a more natural and accurate motion prediction.

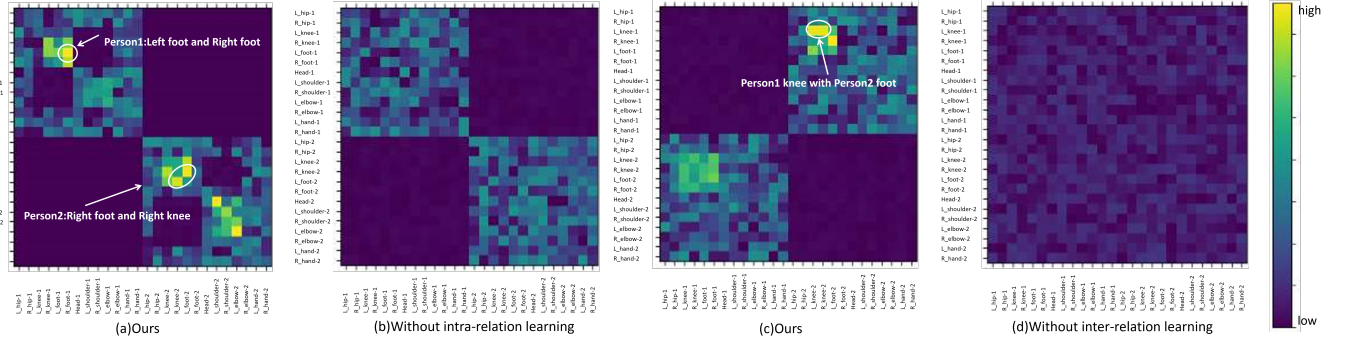


Fig. 12. Attention visualization of intra&inter-relations on 3DPW-RC dataset. We compare our method and baseline without intra-relation or inter-relation modeling. (a) Our method which adopts intra-relation learning. (b) Baseline without intra-relation learning. Lighter colors indicate higher attention scores and higher connections. (c) Our method which adopts inter-relation learning. (d) Baseline without inter-relation learning. Lighter colors indicate higher attention scores and higher connections.

higher compared to those in Fig. 12(b), which lacks the intra-relation learning (The lighter the color, the higher the value). This provides evidence that intra-relation modeling is more conducive to highlighting relations within individual's joints. In Fig. 12(c) and (d), we find that the inter-relation learning significantly differentiates the attention scores among different individuals. This is noticeable in the joints that exhibit large movements when a person performs an action, such as boxing, playing basketball.

G. Ablation Study

In this section, we present the model's complexity and the number of parameters. We also conduct the ablation study on the framework without velocity augment, without intra-relation learning, and without inter-relation learning. The results are shown in Table. IV, Table. V, and Table. VI.

Effectiveness of velocity augment We remove the input of velocity augment and utilize the original position coordinates

as input to verify its validity. The experimental results in Table. V demonstrates that the introduction of velocity information has advantages in modeling the joint-level motion dynamics.

Effectiveness of intra/inter-relation learning We compare our model with other three settings to demonstrate the effectiveness of intra-relation learning and inter-relation learning: i) We only perform inter-relation learning between different individuals ("w/o intra-relation") and remove intra-relation learning; ii) We only capture the individual's intra-relation ("w/o inter-relation") and remove inter-relation learning; iii) We remove the inter/intra-relation learning and adopt a 4-layer Transformer decoder ("w/o intra&inter-relations"). It is obvious that the inter-relation learning and the intra-relation learning are both contribute to the improvement of motion prediction performance.

Effectiveness of loss function. In this section, we perform extensive ablation studies on the 3DPW-RC datasets to investigate the contribution of the different loss functions; see Table

TABLE IV
COMPUTATIONAL COMPLEXITY ANALYSIS ON 3DPW-RC DATASET BASED ON VIM.

Number of Layers $L_i/L_e/L_s$	Parameters (M)	GFLOPs	3DPW-RC					
			AVG	100	240	500	640	900
TBFormer[5]	6.1M	1.7	41.5	10.2	24.0	47.7	55.3	71.4
JRT[45]	6.7M	1.2	39.5	9.5	21.7	44.1	53.4	68.8
Ours $L_1 = 1/L_2 = 3/L_3 = 1$	1.8M	0.5	43.2	10.9	24.5	48.2	57.7	75.1
Ours $L_1 = 2/L_2 = 3/L_3 = 2$	2.4M	0.7	41.5	10.5	23.6	45.5	55.8	72.3
Ours $L_1 = 4/L_2 = 6/L_3 = 4$	4.2M	1.0	39.4	9.3	21.9	44.2	53.8	69.1
Ours $L_1 = 8/L_2 = 13/L_3 = 8$	8.4M	2.1	41.2	10.6	23.3	45.7	55.6	70.9
Ours $L_1 = 8/L_2 = 26/L_3 = 8$	12.1M	2.6	42.3	10.9	24.0	47.0	57.0	72.4
Ours $L_1 = 4/L_2 = 13/L_3 = 4$	5.1M	1.1	39.1	9.2	21.6	43.6	52.6	68.5

TABLE V
ABLATION STUDY OF VELOCITY AUGMENT ON 3DPW-RC BASED ON VIM.

Ablation	3DPW-RC					
	AVG	100	240	500	640	900
w/o velocity	39.6	9.8	22.1	44.7	53.6	69.0
w velocity (Ours)	39.1	9.2	21.6	43.6	52.6	68.5

TABLE VI
ABLATION STUDY OF INTRA/INTER-RELATION MODELING ON 3DPW-RC BASED ON VIM.

Ablation	3DPW-RC					
	AVG	100	240	500	640	900
w/o intra	41.6	10.6	23.3	45.7	55.6	70.9
w/o inter	42.4	10.9	24.0	47.0	57.0	72.4
w/o intra&inter	46.7	12.5	28.6	53.5	62.8	76.3
Ours	39.1	9.2	21.6	43.6	52.6	68.5

VII. We compare our strategy with other three settings: i) only \mathcal{L}_v ; ii) only \mathcal{L}_p ; iii) $\mathcal{L}_p + \mathcal{L}_v$. We see that each loss function can help model get better prediction.

Computational complexity. We evaluate the trade-off between the model's computational cost and performance, as shown in Table. IV. We report the number of parameters and an estimate of the floating operations GFLOPs (Giga Floating-point Operations Per Second) of the models when predict 14 frames (900ms) on 3DPW-RC dataset. Our proposed architecture achieves best performance using $L_1 = 4$ GC-blocks of intra-relation learning, $L_2 = 13$ cross-attention layers of inter-relation learning and $L_3 = 4$ aggregation layers of IAM with 5.1M parameters. Compared to JRT [37] and TBFormer [36], we achieve better performance while using 20% fewer parameters. Additionally, our method achieves near the best results with only 4.2M parameters.

V. CONCLUSION

In this paper, we propose a novel framework for multi-person motion prediction. It aims to avoid undesired and unnatural dependencies between persons by explicitly modeling intra-relations and inter-relations. In addition, we propose a novel plug-and-play aggregation module called the Interaction Aggregation Module (IAM). This module employs an aggregate-attention mechanism to seamlessly integrate intra&inter-relations. Our experiments demonstrate the strong plug-and-play capability of the IAM, and our framework's ability to accurately and naturally predict multi-person 3D motion across the 3DPW, 3DPW-RC, CMU-Mocap, MuPoTS-3D, and synthesized datasets Mix1&Mix2 (9~15 persons).

TABLE VII
ABLATION STUDY OF LOSS FUNCTION.

Ablation	3DPW-RC					
	AVG	100	240	500	640	900
\mathcal{L}_p	39.8	9.5	22.4	45.7	55.6	69.1
\mathcal{L}_v	39.5	9.4	22.1	47.0	57.0	68.9
$\mathcal{L}_p + \mathcal{L}_v$ (Ours)	39.1	9.2	21.6	43.6	52.6	68.5

Nevertheless, our method still have some limitations. Our method mainly focuses on human-to-human interactions in the scene and lacks consideration of the impact of the environments and objects, which is inconsistent with the factors that influence a person's actions in real situations. In future work, we plan to consider the environment and objects to better comply with real-world.

REFERENCES

- [1] A. Gopalakrishnan, A. Mali, D. Kifer, L. Giles, and A. G. Ororbia, "A neural temporal model for human motion prediction," in *Proceedings of the IEEE/CVF Conference on Computer Vision and Pattern Recognition*, 2019, pp. 12 116–12 125.
- [2] J. Shi, J. Zhong, and W. Cao, "Multi-semantics aggregation network based on the dynamic-attention mechanism for 3d human motion prediction," *IEEE Transactions on Multimedia*, vol. 26, pp. 5194–5206, 2024.
- [3] W. Cao, Y. Zhang, J. Gao, A. Cheng, K. Cheng, and J. Cheng, "Pkd: General distillation framework for object detectors via pearson correlation coefficient," *Advances in Neural Information Processing Systems*, vol. 35, pp. 15 394–15 406, 2022.
- [4] D. Zhu, G. Zhai, Y. Di, F. Manhardt, H. Berkemeyer, T. Tran, N. Navab, F. Tombari, and B. Busam, "Ipcc-tp: Utilizing incremental pearson correlation coefficient for joint multi-agent trajectory prediction," in *Proceedings of the IEEE/CVF Conference on Computer Vision and Pattern Recognition*, 2023, pp. 5507–5516.
- [5] X. Peng, S. Mao, and Z. Wu, "Trajectory-aware body interaction transformer for multi-person pose forecasting," in *Proceedings of the IEEE/CVF Conference on Computer Vision and Pattern Recognition*, 2023, pp. 17 121–17 130.
- [6] X. Wang, W. Zhang, C. Wang, Y. Gao, and M. Liu, "Dynamic dense graph convolutional network for skeleton-based human motion prediction," *IEEE Transactions on Image Processing*, vol. 33, pp. 1–15, 2023.
- [7] K. Yi, Q. Zhang, W. Fan, H. He, L. Hu, P. Wang, N. An, L. Cao, and Z. Niu, "Fouriergnn: Rethinking multivariate time series forecasting from a pure graph perspective," *Advances in Neural Information Processing Systems*, vol. 36, 2024.
- [8] S. Zou, Y. Xu, C. Li, L. Ma, L. Cheng, and M. Vo, "Snipper: A spatiotemporal transformer for simultaneous multi-person 3d pose estimation tracking and forecasting on a video snippet," *IEEE Transactions on Circuits and Systems for Video Technology*, 2023.
- [9] A. Saadat, N. Fathi, and S. Saadatanejad, "Towards human pose prediction using the encoder-decoder lstm," in *ICCV Workshops*, 2021.
- [10] S. Ioffe and C. Szegedy, "Batch normalization: Accelerating deep network training by reducing internal covariate shift," in *International conference on machine learning*. pmlr, 2015, pp. 448–456.
- [11] J. L. Ba, J. R. Kiros, and G. E. Hinton, "Layer normalization," *arXiv preprint arXiv:1607.06450*, 2016.

- [12] N. Srivastava, G. Hinton, A. Krizhevsky, I. Sutskever, and R. Salakhutdinov, "Dropout: A simple way to prevent neural networks from overfitting," *Journal of Machine Learning Research*, vol. 15, no. 56, pp. 1929–1958, 2014. [Online]. Available: <http://jmlr.org/papers/v15/srivastava14a.html>
- [13] E. Corona, A. Pumarola, G. Alenyà, and F. Moreno-Noguer, "Context-aware human motion prediction," in *2020 IEEE/CVF Conference on Computer Vision and Pattern Recognition (CVPR)*, 2020, pp. 6990–6999.
- [14] V. Kosaraju, A. Sadeghian, R. Martín-Martín, I. Reid, H. Rezatofighi, and S. Savarese, "Social-bi-gat: Multimodal trajectory forecasting using bicycle-gan and graph attention networks," in *Advances in Neural Information Processing Systems*, H. Wallach, H. Larochelle, A. Beygelzimer, F. d'Alché-Buc, E. Fox, and R. Garnett, Eds., vol. 32. Curran Associates, Inc., 2019.
- [15] Y. Huang, H. Bi, Z. Li, T. Mao, and Z. Wang, "Stgat: Modeling spatial-temporal interactions for human trajectory prediction," in *2019 IEEE/CVF International Conference on Computer Vision (ICCV)*, 2019, pp. 6271–6280.
- [16] T. Lin, Y. Wang, X. Liu, and X. Qiu, "A survey of transformers," *AI Open*, 2022.
- [17] C. Li, H. Yang, and J. Sun, "Intention-interaction graph based hierarchical reasoning networks for human trajectory prediction," *IEEE Transactions on Multimedia*, pp. 1–12, 2022.
- [18] Z. Li, Y. Li, L. Tang, T. Zhang, and J. Su, "Two-person graph convolutional network for skeleton-based human interaction recognition," *IEEE Transactions on Circuits and Systems for Video Technology*, vol. 33, no. 7, pp. 3333–3342, 2023.
- [19] W. Guo, X. Bie, X. Alameda-Pineda, and F. Moreno-Noguer, "Multi-person extreme motion prediction," in *Proceedings of the IEEE/CVF Conference on Computer Vision and Pattern Recognition*, 2022, pp. 13 053–13 064.
- [20] S. Saadatnejad, A. Rasekh, M. Mofayez, Y. Medghalchi, S. Rajabzadeh, T. Mordan, and A. Alahi, "A generic diffusion-based approach for 3d human pose prediction in the wild," in *2023 IEEE International Conference on Robotics and Automation (ICRA)*. IEEE, 2023, pp. 8246–8253.
- [21] H. Joo, T. Simon, X. Li, H. Liu, L. Tan, L. Gui, S. Banerjee, T. Godisart, B. Nabbe, I. Matthews, T. Kanade, S. Nobuhara, and Y. Sheikh, "Panoptic studio: A massively multiview system for social interaction capture," 2016.
- [22] W. Li, H. Liu, R. Ding, M. Liu, P. Wang, and W. Yang, "Exploiting temporal contexts with strided transformer for 3d human pose estimation," *IEEE Transactions on Multimedia*, vol. 25, pp. 1282–1293, 2022.
- [23] W. Jiang, N. Kolotouros, G. Pavlakos, X. Zhou, and K. Daniilidis, "Coherent reconstruction of multiple humans from a single image," in *CVPR*, 2020.
- [24] M. Hassan, V. Choutas, D. Tzionas, and M. Black, "Resolving 3d human pose ambiguities with 3d scene constraints," in *Proceedings of the IEEE/CVF International Conference on Computer Vision*, 2019, p. 2282–2292.
- [25] J. Liu, X. Wang, C. Wang, Y. Gao, and M. Liu, "Temporal decoupling graph convolutional network for skeleton-based gesture recognition," *IEEE Transactions on Multimedia*, vol. 26, pp. 811–823, 2023.
- [26] S. Hochreiter and J. Schmidhuber, "Long short-term memory," *Neural Computation*, vol. 9, no. 8, pp. 1735–1780, 1997.
- [27] P. Veličković, G. Cucurull, A. Casanova, A. Romero, P. Liò, and Y. Bengio, "Graph attention networks," 2018.
- [28] V. Adeli, E. Adeli, I. Reid, J. C. Niebles, and H. Rezatofighi, "Socially and contextually aware human motion and pose forecasting," *IEEE Robotics and Automation Letters*, vol. 5, no. 4, pp. 6033–6040, 2020.
- [29] X. Nie, X. Chen, H. Jin, Z. Zhu, Y. Yan, and D. Qi, "Triplet attention transformer for spatiotemporal predictive learning," *arXiv preprint arXiv:2310.18698*, 2023.
- [30] E. Aksan, M. Kaufmann, P. Cao, and O. Hilliges, "A spatio-temporal transformer for 3d human motion prediction," in *2021 International Conference on 3D Vision (3DV)*. IEEE, 2021, pp. 565–574.
- [31] W. Mao, M. Liu, and M. Salzmann, "History repeats itself: Human motion prediction via motion attention," in *Computer Vision—ECCV 2020: 16th European Conference, Glasgow, UK, August 23–28, 2020, Proceedings, Part XIV 16*. Springer, 2020, pp. 474–489.
- [32] P. Ghosh, J. Song, E. Aksan, and O. Hilliges, "Learning human motion models for long-term predictions," in *2017 International Conference on 3D Vision (3DV)*. IEEE, 2017, pp. 458–466.
- [33] L. Dang, Y. Nie, C. Long, Q. Zhang, and G. Li, "Msr-gcn: Multi-scale residual graph convolution networks for human motion prediction," in *Proceedings of the IEEE/CVF International Conference on Computer Vision*, 2021, pp. 11 467–11 476.
- [34] C. Chen, Y. Liu, S. Kreiss, and A. Alahi, "Crowd-robot interaction: Crowd-aware robot navigation with attention-based deep reinforcement learning," in *2019 international conference on robotics and automation (ICRA)*. IEEE, 2019, pp. 6015–6022.
- [35] T.-H. Vu, S. Ambellouis, J. Boonaert, and A. Taleb-Ahmed, "Anomaly detection in surveillance videos by future appearance-motion prediction," in *VISIGRAPP (5: VISAPP)*, 2020, pp. 484–490.
- [36] S. Fang, Z. Wang, Y. Zhong, J. Ge, and S. Chen, "Tbp-former: Learning temporal bird's-eye-view pyramid for joint perception and prediction in vision-centric autonomous driving," in *Proceedings of the IEEE/CVF Conference on Computer Vision and Pattern Recognition*, 2023, pp. 1368–1378.
- [37] C. Xu, M. Li, Z. Ni, Y. Zhang, and S. Chen, "Groupnet: Multiscale hypergraph neural networks for trajectory prediction with relational reasoning," in *Proceedings of the IEEE/CVF Conference on Computer Vision and Pattern Recognition*, 2022, pp. 6498–6507.
- [38] H. Wang, J. Dong, B. Cheng, and J. Feng, "Pvred: A position-velocity recurrent encoder-decoder for human motion prediction," *IEEE Transactions on Image Processing*, vol. 30, pp. 6096–6106, 2021.
- [39] C. Zhong, L. Hu, Z. Zhang, Y. Ye, and S. Xia, "Spatio-temporal gating-adjacency gcn for human motion prediction," in *Proceedings of the IEEE/CVF Conference on Computer Vision and Pattern Recognition*, 2022, pp. 6447–6456.
- [40] T. Sofianos, A. Sampieri, L. Franco, and F. Galasso, "Space-time-separable graph convolutional network for pose forecasting," in *Proceedings of the IEEE/CVF International Conference on Computer Vision*, 2021, pp. 11 209–11 218.
- [41] C. Ionescu, D. Papava, V. Olaru, and C. Sminchisescu, "Human3.6m: Large scale datasets and predictive methods for 3d human sensing in natural environments," *IEEE Transactions on Pattern Analysis and Machine Intelligence*, vol. 36, no. 7, pp. 1325–1339, 2014.
- [42] V. Adeli, M. Ehsanpour, I. Reid, J. C. Niebles, S. Savarese, E. Adeli, and H. Rezatofighi, "Tripod: Human trajectory and pose dynamics forecasting in the wild," in *2021 IEEE/CVF International Conference on Computer Vision (ICCV)*, 2021, pp. 13 370–13 380.
- [43] J. Wang, H. Xu, M. Narasimhan, and X. Wang, "Multi-person 3d motion prediction with multi-range transformers," *Advances in Neural Information Processing Systems*, vol. 34, pp. 6036–6049, 2021.
- [44] E. Vendrow, S. Kumar, E. Adeli, and H. Rezatofighi, "Somoformer: Multi-person pose forecasting with transformers," 2022.
- [45] Q. Xu, W. Mao, J. Gong, C. Xu, S. Chen, W. Xie, Y. Zhang, and Y. Wang, "Joint-relation transformer for multi-person motion prediction," in *Proceedings of the IEEE/CVF International Conference on Computer Vision*, 2023, pp. 9816–9826.
- [46] T. von Marcard, R. Henschel, M. J. Black, B. Rosenhahn, and G. Pons-Moll, "Recovering accurate 3d human pose in the wild using imus and a moving camera," in *Proceedings of the European Conference on Computer Vision (ECCV)*, September 2018.
- [47] C. Wang, Y. Wang, Z. Huang, and Z. Chen, "Simple baseline for single human motion forecasting," in *Proceedings of the IEEE/CVF International Conference on Computer Vision*, 2021, pp. 2260–2265.
- [48] J. Bütepage, H. Kjellström, and D. Kragic, "Anticipating many futures: Online human motion prediction and generation for human-robot interaction," in *2018 IEEE International Conference on Robotics and Automation (ICRA)*, 2018, pp. 4563–4570.
- [49] V. Adeli, E. Adeli, I. Reid, J. C. Niebles, and H. Rezatofighi, "Socially and contextually aware human motion and pose forecasting," *IEEE Robotics and Automation Letters*, vol. 5, no. 4, pp. 6033–6040, 2020.
- [50] Z. Cao, H. Gao, K. Mangalam, Q.-Z. Cai, M. Vo, and J. Malik, "Long-term human motion prediction with scene context," in *Computer Vision – ECCV 2020*, A. Vedaldi, H. Bischof, T. Brox, and J.-M. Frahm, Eds. Cham: Springer International Publishing, 2020, pp. 387–404.
- [51] "CMU Graphics Lab Motion Capture Database," <http://mocap.cs.cmu.edu/>.
- [52] D. Mehta, O. Sotnychenko, F. Mueller, W. Xu, S. Sridhar, G. Pons-Moll, and C. Theobalt, "Single-shot multi-person 3d pose estimation from monocular rgb," in *2018 International Conference on 3D Vision (3DV)*. IEEE, 2018, pp. 120–130.
- [53] I. Loshchilov and F. Hutter, "Decoupled weight decay regularization," *arXiv preprint arXiv:1711.05101*, 2017.
- [54] D. Wu and L. Shao, "Leveraging hierarchical parametric networks for skeletal joints based action segmentation and recognition," in *Proceedings of the IEEE conference on computer vision and pattern recognition*, 2014, pp. 724–731.

- [55] C. Liu and Y. Mu, "Multi-granularity interaction for multi-person 3d motion prediction," *IEEE Transactions on Circuits and Systems for Video Technology*, vol. 34, no. 3, pp. 1546–1558, 2024.
- [56] T. Ma, Y. Nie, C. Long, Q. Zhang, and G. Li, "Progressively generating better initial guesses towards next stages for high-quality human motion prediction," in *Proceedings of the IEEE/CVF Conference on Computer Vision and Pattern Recognition*, 2022, pp. 6437–6446.
- [57] J. Tang, J. Zhang, R. Ding, B. Gu, and J. Yin, "Collaborative multi-dynamic pattern modeling for human motion prediction," *IEEE Transactions on Circuits and Systems for Video Technology*, vol. 33, no. 8, pp. 3689–3700, 2023.
- [58] N. Mahmood, N. Ghorbani, N. F. Troje, G. Pons-Moll, and M. J. Black, "AMASS: archive of motion capture as surface shapes," *CoRR*, vol. abs/1904.03278, 2019. [Online]. Available: <http://arxiv.org/abs/1904.03278>
- [59] W. Mao, M. Liu, M. Salzmann, and H. Li, "Learning trajectory dependencies for human motion prediction," in *Proceedings of the IEEE/CVF international conference on computer vision*, 2019, pp. 9489–9497.
- [60] B. Parsaeifard, S. Saadatnejad, Y. Liu, T. Mordan, and A. Alahi, "Learning decoupled representations for human pose forecasting," in *Proceedings of the IEEE/CVF International Conference on Computer Vision*, 2021, pp. 2294–2303.
- [61] B. Tang, Y. Zhong, C. Xu, W.-T. Wu, U. Neumann, Y. Zhang, S. Chen, and Y. Wang, "Collaborative uncertainty benefits multi-agent multi-modal trajectory forecasting," *IEEE Transactions on Pattern Analysis and Machine Intelligence*, 2023.
- [62] H. Yu, X. Fan, Y. Hou, W. Pei, H. Ge, X. Yang, D. Zhou, Q. Zhang, and M. Zhang, "Toward realistic 3d human motion prediction with a spatio-temporal cross- transformer approach," *IEEE Transactions on Circuits and Systems for Video Technology*, vol. 33, no. 10, pp. 5707–5720, 2023.
- [63] R. X. Gao, L. Wang, P. Wang, J. Zhang, and H. Liu, "Human motion recognition and prediction for robot control," in *Advanced Human-Robot Collaboration in Manufacturing*. Springer, 2021, pp. 261–282.
- [64] C. Xu, W. Mao, W. Zhang, and S. Chen, "Remember intentions: Retrospective-memory-based trajectory prediction," in *Proceedings of the IEEE/CVF Conference on Computer Vision and Pattern Recognition*, 2022, pp. 6488–6497.